

Sub-Planck phase-space structures and Heisenberg-limited measurements

F. Toscano,¹ D. A. R. Dalvit,² L. Davidovich,¹ and W. H. Zurek²

¹*Instituto de Física, Universidade Federal do Rio de Janeiro, Caixa Postal 68.528, 21.941-972, Rio de Janeiro, Brazil*

²*Theoretical Division, MS B213, Los Alamos National Laboratory, Los Alamos, New Mexico 87545, USA*

(Received 10 August 2005; revised manuscript received 12 December 2005; published 6 February 2006)

We show how sub-Planck phase-space structures in the Wigner function [W. H. Zurek, *Nature (London)* **412**, 712 (2001)] can be used to achieve Heisenberg-limited sensitivity in weak-force measurements. Nonclassical states of harmonic oscillators, consisting of superpositions of coherent states, are shown to be useful for the measurement of weak forces that cause translations or rotations in phase space, which is done by entangling the quantum oscillator with a two-level system. Implementations of this strategy in cavity QED and ion traps are described.

DOI: [10.1103/PhysRevA.73.023803](https://doi.org/10.1103/PhysRevA.73.023803)

PACS number(s): 42.50.Dv, 03.65.-w, 42.50.Pq, 42.50.Vk

INTRODUCTION

Quantum metrology encompasses the estimation of an unknown parameter of a quantum system, and has been the subject of increasing scientific and technological interest due to enhanced measurement techniques allowed by quantum mechanics [1]. The two typical problems of small quantum parameter estimation are high-precision phase measurements and the detection of weak forces [2]. Detection of a small relative phase between two superposed quantum states includes two equivalent techniques, i.e., Ramsey spectroscopy and Mach-Zehnder interferometry [3,4]. They involve detection of a rotation of the quantum state in phase space around the origin. Thus, the problem of phase determination is ultimately associated with the estimation of a small rotation angle. Detection of weak forces can be traced back to the pioneering work on gravitational wave detectors that proposed to use a quantum-mechanical oscillator as an antenna [5,6]. A weak force (exerted, e.g., by the wave) induces a displacement of the quantum state in phase space in some direction. Thus, in this case the quantum parameter estimation can be reduced to the determination of a small linear displacement.

The precision in quantum parameter estimation depends on the energy resources (e.g., the average number \bar{n} of photons) involved in the measurement process. It is well known that using quasiclassical states the sensitivity is at the standard quantum limit (SQL), also known as the shot-noise limit. In particular, coherent states are associated with SQL: The phase-space size of a coherent state is given by $\approx \sqrt{\hbar}$ and its distance from the origin is $\approx \sqrt{\hbar\bar{n}}$. The smallest noticeable rotation that will lead to approximate orthogonality is equal to its angular size as “seen from the origin,” $\sqrt{\hbar}/\sqrt{\hbar\bar{n}} \approx \bar{n}^{-1/2}$, i.e., the standard quantum limit (see Fig. 1). The same argument implies that the smallest detectable displacement is of the order of $\sqrt{\hbar}$, so the SQL for weak-force detection is independent of \bar{n} , i.e., it scales as \bar{n}^0 . The SQL limit can be surpassed by using quantum effects (such as entanglement and squeezing), reaching the so-called Heisenberg limit (HL), in which the sensitivity is higher than the SQL by $\bar{n}^{-1/2}$ [4,7–9]. Sub-shot-noise sensitivities, approaching the ultimate Heisenberg limit, can be achieved using

path-entangled states of photons [10–16] or ions [17–19], recently produced in experiments.

In this paper we show that, as is already anticipated by the brief discussion of the SQL above, the sensitivity of the quantum state to displacements is related to the smallest phase-space structures associated with its Wigner function W . This connection was conjectured by one of us [20] in the context of the discussion of the sub-Planck structures in W . The area of these structures can be as small as $a = \hbar^2/A$, where A is the action of the effective support of W . A is limited from above by the classical action of the state, but it can be much smaller than that. It is least for a coherent state, i.e., $A \approx \hbar$, which yields $a = \hbar^2/\hbar = \hbar$, and then leads to the SQL. Sub-SQL sensitivities can be achieved with coherent squeezed states [21], which also have $A \approx \hbar$ but, contrary to coherent states, have unequal quadratures: one is contracted proportionally to $\sqrt{\hbar}e^{-r}$, and the other is expanded proportionally to $\sqrt{\hbar}e^r$ ($r > 0$ is the squeezing parameter). Thus, squeezed states have sub-shot-noise sensitivity for perturbations acting along the squeezed direction. However, for a fixed \bar{n} , we shall show that states with much larger values of $A \approx \hbar\bar{n}$ can be found, which exhibit sensitivity set by $\sqrt{a} \approx \sqrt{\hbar/\bar{n}}$ to displacements; this then allows one to saturate the Heisenberg limit. In this way, we shall demonstrate that

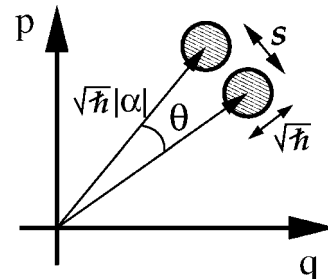


FIG. 1. Phase-space representation of the standard quantum limit for rotations. Coherent states have phase-space size of the order $\varepsilon \approx \sqrt{\hbar}$. A coherent state of complex amplitude $\sqrt{\hbar}\alpha$ is rotated around the origin by a small angle θ . The initial and final coherent states are distinguishable (approximately orthogonal) when the linear displacement $\varepsilon \approx s \approx \sqrt{\hbar}|\alpha|\theta$, which leads to SQL sensitivity for rotations $\theta \approx 1/|\alpha| = 1/\sqrt{\bar{n}}$.

the sub-Planck-scale \hbar^2/A determines the sensitivity of small parameter estimation.

Our paper is organized as follows. In the next section we explain the connection between sub-Planck phase-space structures and Heisenberg-limited sensitivity in quantum metrology. In the following section we discuss a general scheme for measuring small displacements and rotations in phase space by using nonclassical states of a harmonic oscillator, suitably coupled to a two-level system (TLS). We describe in the next section how to implement our proposal in both cavity QED and ion-trap experiments, which can take advantage of sub-Planck structures for quantum-enhanced measurements. Finally, we present our conclusions.

SUB-PLANCK STRUCTURES FOR QUANTUM METROLOGY

Let us consider superpositions of M coherent states, equidistantly placed on a circle \mathcal{C} of radius $|\alpha| \gg 1$,

$$|\text{cat}_M\rangle = \frac{1}{\sqrt{M}} \sum_{k=1}^M e^{i\gamma_k} |e^{i\varphi_k}\alpha\rangle, \quad (1)$$

where $\varphi_k = 2\pi k/M$, and the γ_k 's are arbitrary phases. These ‘‘circular states’’ are nonclassical states of a harmonic oscillator for which the mean number of excitations is $\bar{n} \equiv \langle \text{cat}_M | \hat{a}^\dagger \hat{a} | \text{cat}_M \rangle \approx |\alpha|^2$. States of the form (1) include the periodic case of the ‘‘generalized coherent states’’ considered in [22,23]. These nonclassical states can be generated by nonlinear optical processes [24,25], and by quantum-nondemolition measurements of the photon number in cavity QED [26] or the vibrational number of a trapped ion [27]. Some properties of these states were studied in [28,29]. Examples are the Schrödinger cat (macroscopic superposition) state

$$|\text{cat}_2\rangle = (|\alpha\rangle + |-\alpha\rangle)/\sqrt{2}, \quad (2)$$

and the compass state [20]

$$|\text{compass}\rangle = |\text{cat}_4\rangle = (|\alpha\rangle + |-\alpha\rangle + |i\alpha\rangle + |-i\alpha\rangle)/2. \quad (3)$$

We show in the following that when a unitary perturbation \hat{U}_x induces a small linear displacement of magnitude x , the overlap between the unperturbed state $|\text{cat}_M\rangle$ and the perturbed one $|\text{cat}_M(x)\rangle = \hat{U}_x |\text{cat}_M\rangle$ oscillates with a typical frequency $\sim |\alpha|$. Therefore, the least linear displacement $x=s$ needed to distinguish the two states is $s \sim 1/|\alpha|$. This scale defines the Heisenberg limit for displacement measurement. In the case of a rotation $x=\theta$, quasiorthogonality occurs when the rotation induces a linear displacement of the center of the circle \mathcal{C} of the order of $s \sim \theta|\alpha|$, with $s \sim 1/|\alpha|$. Therefore, the detectable angle is $\theta \sim 1/|\alpha|^2$, defining in this case the Heisenberg limit for rotation measurements. We also show that the oscillatory behavior of the overlap function $|\langle \text{cat}_M | \text{cat}_M(x) \rangle|^2$ has its origin in the overlap between the oscillatory structure of the Wigner functions of the unperturbed and the perturbed states whose typical frequency of their oscillations is precisely proportional to $|\alpha|$. Thus, we prove that the sub-Planck phase-space structure of the states

in Eq. (1) determines its Heisenberg-limited sensitivity for quantum metrology applications.

Displacements

We consider a small linear displacement given by the unitary operator $\hat{D}(\beta) \equiv e^{\beta \hat{a}^\dagger - \beta^* \hat{a}}$ in an arbitrary direction $\beta = e^{i\varphi} \alpha s / |\alpha|$ with magnitude $|\beta| = s \ll 1$. This operation transforms the unperturbed state $|\text{cat}_M\rangle$ into the perturbed state $|\text{cat}_M(s)\rangle \equiv \hat{D}(\beta) |\text{cat}_M\rangle$. The overlap between these two states can be calculated as the integral over phase space $\bar{\alpha}$ of the overlap between their respective Wigner functions,

$$|\langle \text{cat}_M | \text{cat}_M(s) \rangle|^2 = \int \frac{d^2\bar{\alpha}}{\pi} W_{|\text{cat}_M\rangle}(\bar{\alpha}) W_{|\text{cat}_M(s)\rangle}(\bar{\alpha}). \quad (4)$$

The Wigner function $W_{|\text{cat}_M(s)\rangle}(\bar{\alpha})$ of the perturbed state is

$$W_{|\text{cat}_M(s)\rangle}(\bar{\alpha}) = \frac{1}{M} \sum_{k=1}^M \sum_{l=1}^M e^{i(\gamma_k - \gamma_l)} e^{i s a_{kl} |\alpha|} W_{kl}^s(\bar{\alpha}), \quad (5)$$

where W_{kl}^s are the Weyl-Wigner functions [30,31] corresponding to the operators $|e^{i\varphi_k}\alpha + \beta\rangle \langle e^{i\varphi_l}\alpha + \beta|$, and $a_{kl} \equiv \sin(\varphi - \varphi_k) - \sin(\varphi - \varphi_l)$. The Wigner function $W_{|\text{cat}_M\rangle}(\bar{\alpha})$ of the unperturbed state is obtained from Eq. (5) by setting $s=0$. The resulting Weyl-Wigner functions $W_{kl} \equiv W_{kl}^{s=0}$ are

$$\begin{aligned} W_{kl}(\bar{\alpha}) = & 2 \exp \left[-2 \left| \bar{\alpha} - \left(\frac{\alpha_k + \alpha_l}{2} \right) \right|^2 \right] \\ & \times \exp[i2 \text{Im}[-(e^{-i\varphi_k} - e^{-i\varphi_l}) \alpha^* \bar{\alpha}]] \\ & \times \exp[i2 \text{Im}(e^{i(\varphi_l - \varphi_k)} |\alpha|^2)]. \end{aligned} \quad (6)$$

Therefore, the Wigner function $W_{|\text{cat}_M\rangle}$ of the unperturbed state consists of M Gaussian functions W_{kk} centered at the phase-space points $e^{i\varphi_k}\alpha$, plus interference terms W_{kl} ($l \neq k$) which oscillate with a typical frequency $\propto |\alpha|$ (see Fig. 2).

Expressing the overlap Eq. (4) in terms of the Weyl-Wigner functions and using that $|\alpha| \gg 1$ we get

$$\begin{aligned} |\langle \text{cat}_M | \text{cat}_M(s) \rangle|^2 & \approx \frac{1}{M^2} \left[\sum_{k=1}^M \int \frac{d\bar{\alpha}^2}{\pi} W_{kk}(\bar{\alpha}) W_{kk}^s(\bar{\alpha}) \right. \\ & \left. + \sum_{k=1}^M \sum_{l>k}^M 2 \text{Re} \left(e^{i a_{kl} |\alpha| s} \int \frac{d\bar{\alpha}^2}{\pi} W_{lk}(\bar{\alpha}) W_{kl}^s(\bar{\alpha}) \right) \right]. \end{aligned} \quad (7)$$

Here we have neglected contributions $\int (d\bar{\alpha}^2/\pi) W_{lk}(\bar{\alpha}) W_{k'l'}^s(\bar{\alpha}) \approx O(e^{-|\alpha|^2})$ for $l \neq l'$ and $k \neq k'$. A further simplification can be achieved using the fact that the perturbation is small, $|\beta| = s \ll 1$. Indeed, in this case we have $\hat{D}(\beta) |\alpha\rangle = e^{i \text{Im}(\beta \alpha^*)} |\alpha + \beta\rangle \approx e^{2i \text{Im}(\beta \alpha^*)} |\alpha\rangle$, so that the perturbed and unperturbed Weyl-Wigner functions are related as

$$W_{kl}^s(\bar{\alpha}) \approx e^{i s a_{kl} |\alpha|} W_{kl}(\bar{\alpha}). \quad (8)$$

Therefore, the integral in the first term of Eq. (7) is equal to 1, and the integral of the second term is equal to $e^{i s a_{kl} |\alpha|}$. Finally, the overlap reads

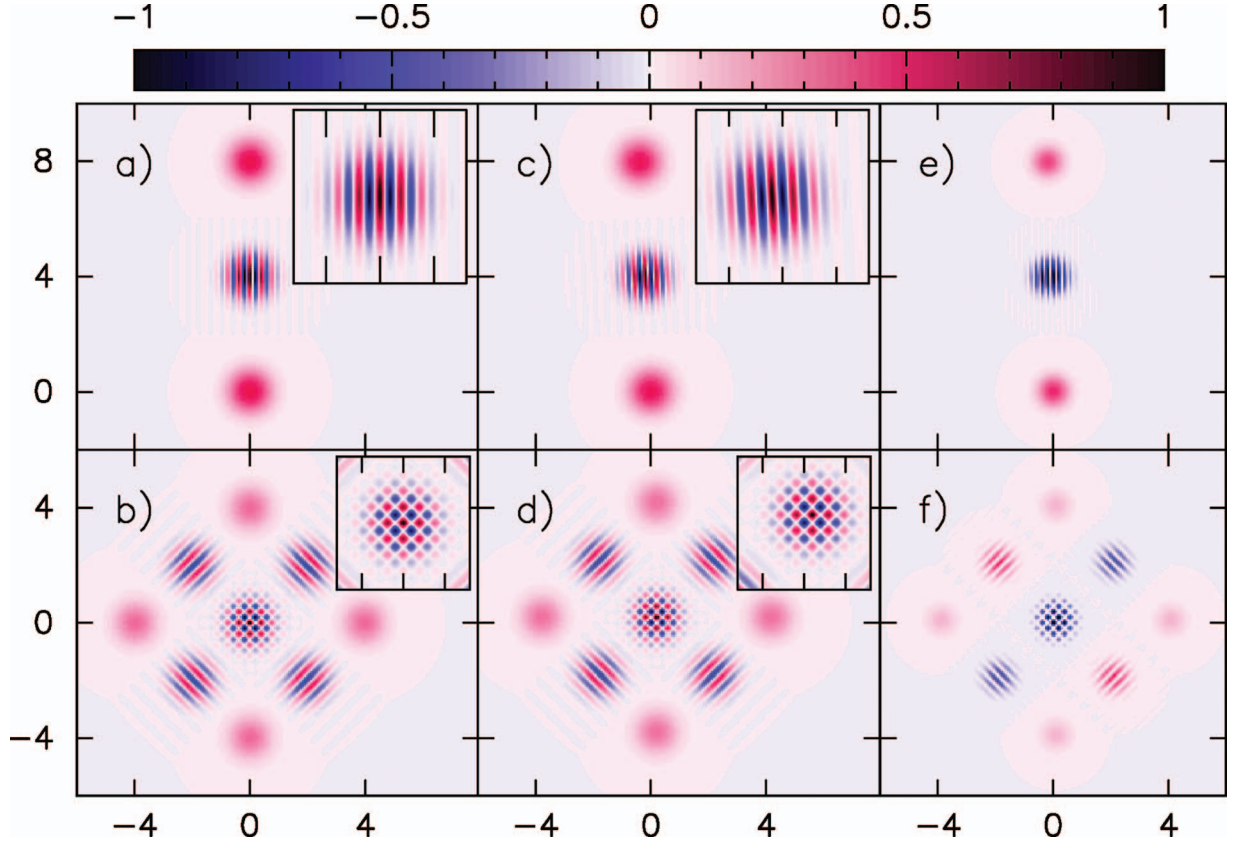


FIG. 2. (Color) The Wigner functions in the α plane for: (a) the displaced cat state $|\overline{\text{cat}}_2\rangle \equiv \hat{D}(\alpha)|\text{cat}_2\rangle$, and (b) the compass state $|\overline{\text{compass}}\rangle$ for $\alpha=4i$. The displaced cat state is quasiorthogonal to the rotated state $\hat{R}(\theta)|\overline{\text{cat}}_2\rangle$ ($\theta=\pi/4|\alpha|^2$) in (c) at the Heisenberg limit scale $\theta\sim 1/|\alpha|^2$. The compass state is quasiorthogonal to the translated compass state $\hat{D}(\beta)|\overline{\text{compass}}\rangle$ ($\beta=e^{i\pi/4}\pi/2\sqrt{2}|\alpha|$) in (d) at the Heisenberg limit scale $|\beta|\sim 1/|\alpha|$. The insets enlarge the central interference pattern of the displayed Wigner functions. In (e) and (f) we display the respective products of the unperturbed and perturbed Wigner functions. When performing the integration over the α plane, the negative contributions (in blue) cancel the positive ones (in red), leading to quasiorthogonality.

$$|\langle \text{cat}_M | \text{cat}_M(s) \rangle|^2 \approx \frac{1}{M^2} \left(M + \sum_{k=1}^M \sum_{l>k}^M 2 \cos(2s a_{kl} |\alpha|) \right). \quad (9)$$

We see that the oscillations in the function $|\langle \text{cat}_M | \text{cat}_M(s) \rangle|^2$ come from the overlap between the interference patterns W_{kl} and W_{kl}^s ($l \neq k$) of the Wigner functions of the unperturbed and perturbed states, respectively. The typical frequency of these oscillations is proportional to $|\alpha|$, and implies that the states $|\text{cat}_M\rangle$ are Heisenberg-limited sensitive to displacements ($s \sim 1/|\alpha|$). Similar oscillations when the initial state is a Fock state were discussed in [32].

Rotations

Small rotations in phase space, induced by the operator $\hat{R}(\theta) = e^{i\theta \hat{a}^\dagger \hat{a}}$, with $\theta \ll 1$, can be treated in a similar way. It is first necessary to displace the state $|\text{cat}_M\rangle$ so that the displaced circle \mathcal{C} contains the origin of phase space. This can be achieved by considering the displaced state $|\overline{\text{cat}}_M\rangle \equiv \hat{D}(\eta)|\text{cat}_M\rangle$, with $\eta=\alpha$. If we now rotate this displaced state in an angle θ around the origin we obtain

$$\hat{R}(\theta)|\overline{\text{cat}}_M\rangle \approx \frac{e^{2i\theta|\alpha|^2}}{\sqrt{M}} \sum_{k=1}^M e^{i(\gamma_k + 2\theta|\alpha|^2 b_k)} |e^{i\varphi_k} \alpha + \eta\rangle, \quad (10)$$

where $b_k \equiv \cos(\varphi_k) - \sin(\varphi_k)$. To obtain this equation we have used that, in the limit $\theta \ll 1/2|\alpha|$, we have $\hat{R}(\theta)|\alpha\rangle = |e^{i\theta}\alpha\rangle \approx |\alpha + i\theta\alpha\rangle$, and $\hat{D}(\beta)|\alpha\rangle \approx e^{2i \text{Im}(\beta\alpha^*)} |\alpha\rangle$. The state given in Eq. (10) is the same one obtains by applying a linear displacement β to the state $|\overline{\text{cat}}_M\rangle$ provided that β is orthogonal to η (i.e., $\beta = i\eta s/|\eta|$), and has a magnitude $|\beta|=s=|\alpha|\theta \ll 1$. Then, the overlap function between the displaced state $|\overline{\text{cat}}_M\rangle$ and the corresponding rotated state $|\overline{\text{cat}}_M(\theta)\rangle \equiv \hat{R}(\theta)|\overline{\text{cat}}_M\rangle$ is

$$|\langle \overline{\text{cat}}_M | \overline{\text{cat}}_M(\theta) \rangle|^2 \approx |\langle \overline{\text{cat}}_M | \hat{D}(\beta) | \overline{\text{cat}}_M \rangle|^2 = |\langle \text{cat}_M | \hat{D}(\beta) | \text{cat}_M \rangle|^2. \quad (11)$$

The last overlap of this equation is given by Eq. (9) with $s=\theta|\alpha|$ (see Fig. 1). This shows that the displaced states $|\overline{\text{cat}}_M\rangle$ are HL sensitive to rotations ($\theta \sim 1/|\alpha|^2$).

MEASUREMENT STRATEGY

Let us consider the simplest case with $M=2$, i.e., the cat state $|\text{cat}_2\rangle$. After a small displacement $\beta=i\alpha s/|\alpha|$, in a direction orthogonal to α (which is the direction of maximum-sensitivity), the overlap function according to Eq. (9) is

$$|\langle \text{cat}_2 | \text{cat}_2(s) \rangle|^2 \approx [1 + \cos(4|\alpha|s)]/2. \quad (12)$$

As we have seen, this is also the overlap function when we consider a small rotation, of angle $\theta=s/|\alpha|$, applied to the state $|\overline{\text{cat}}_2\rangle \equiv \hat{D}(\alpha)|\text{cat}_2\rangle = (1/\sqrt{2})(|2\alpha\rangle + |0\rangle)$. We see that if we could measure these overlap functions, we could determine the parameters s or $\theta=s/|\alpha|$ at the Heisenberg limit, i.e., with a sensitivity proportional to $1/|\alpha|$ and $1/|\alpha|^2$, respectively. It should be noted that the $M>2$ generalized coherent states, such as the compass state ($M=4$), have sub-Planck structures that lead to HL sensitivity for displacements in any direction β . The cat state, however, has minimal (zero) sensitivity for displacements along the direction α .

The measurement of the small perturbations can be realized by entangling the system with a two-level system. The general method is the following. We initially prepare the oscillator in a large-amplitude coherent state $|\alpha\rangle$, and the TLS in one of its two states, say in the upper state $|e\rangle$. The composite system is then evolved during a certain time $t=T$ under a unitary evolution \hat{U} , which includes the interaction of the oscillator with the TLS as well as possible additional unitary operations acting only either on the states of the oscillator or on those of the TLS. The unitary perturbation \hat{U}_x is then applied to the oscillator (assuming that it does not affect the state of the TLS), and finally the unitary evolution \hat{U} is undone. The final entangled state of the composite system is

$$|\Psi_f\rangle = \hat{U}^\dagger(T)\hat{U}_x\hat{U}(T)|e, \alpha\rangle = \sqrt{P_e}|e, \Psi_S^e\rangle + \sqrt{P_g}|g, \Psi_S^g\rangle, \quad (13)$$

where P_e and $P_g=1-P_e$ are the probabilities of measuring the TLS in levels e and g , respectively. The unitary operator \hat{U} must be such that the intermediate states $|\Psi\rangle = \hat{U}|e, \alpha\rangle$ and $|\Phi\rangle = \hat{U}_x\hat{U}|e, \alpha\rangle$ verify $|\langle \Psi | \Phi \rangle|^2 \approx |\langle \text{cat}_M | \text{cat}_M(x) \rangle|^2$. Given that $|\langle e, \alpha | \Psi_f \rangle|^2 = |\langle \Psi | \Phi \rangle|^2$, the information about the perturbation parameter x , contained in the overlap function $|\langle \text{cat}_M | \text{cat}_M(x) \rangle|^2$, is then translated into the probabilities, i.e.,

$$P_e = 1 - P_g = \frac{|\langle e, \alpha | \Psi_f \rangle|^2}{|\langle \alpha | \Psi_S^e \rangle|^2} \approx \frac{|\langle \text{cat}_M | \text{cat}_M(x) \rangle|^2}{|\langle \alpha | \Psi_S^e \rangle|^2}. \quad (14)$$

The method proposed above can also be used to measure the Loschmidt echo, which quantifies the sensitivity of a quantum system to perturbations [33–36].

CAVITY QED AND ION-TRAP IMPLEMENTATIONS

The strategy of measuring small perturbations on superpositions of coherent states of quantum harmonic oscillators via two-level systems can be implemented in cavity QED and ion-trap experiments. In the following we describe in

detail all the necessary steps for the implementation of the cat state ($M=2$). Similar strategies can be used for higher ($M>2$) generalized coherent states. For example, the compass state can be generated in ion traps by means of engineering the ion-laser interaction in order to realize a nonlinear multiquantum Jaynes-Cummings dynamics. This will be the subject of a future publication [37].

Let us consider the interaction between a harmonic oscillator mode and a two-level system as given by the Jaynes-Cummings (JC) model [38]. In a cavity QED scenario [26,39], the harmonic oscillator is a single mode of the quantized electromagnetic field in the cavity and the TLS is a Rydberg atom with a two-level electronic transition coupled to the field through the JC evolution. In an ion-trap scenario [40], the harmonic oscillator corresponds to the center-of-mass motion of the trapped ion, and it couples to the TLS (which corresponds to an internal atomic transition) when the ion is irradiated by a laser. In the following we adopt the cavity QED scenario, adding short remarks on issues that may be specific for trapped-ion implementations.

The coherent dynamics in the JC model is described by the Hamiltonian

$$\hat{H}_{JC} = \hat{H}_A + \hat{H}_F + \hat{H}_{AF}, \quad (15)$$

where $\hat{H}_A = (\hbar\omega_0/2)\hat{\sigma}_z$ is the atomic TLS Hamiltonian, with $\hat{\sigma}_z \equiv |e\rangle\langle e| - |g\rangle\langle g|$, and ω_0 is the transition frequency between the lower $|g\rangle$ and the upper $|e\rangle$ states. The harmonic field mode is described by $\hat{H}_F \equiv \hbar\omega\hat{a}^\dagger\hat{a}$ and the interaction Hamiltonian is $\hat{H}_{AF} \equiv (\hbar\Omega_0/2)(\hat{\sigma}^\dagger\hat{a} + \hat{\sigma}\hat{a}^\dagger)$ where $\hat{\sigma} = |g\rangle\langle e|$ and Ω_0 is the vacuum Rabi frequency. It is more convenient to use the interaction picture with respect to the free evolution $\hat{H}_A + \hat{H}_F$, so the JC dynamics is described by

$$\hat{H}_{AF}^I = (\hbar\Omega_0/2)(e^{i\delta t}\hat{\sigma}^\dagger\hat{a} + e^{-i\delta t}\hat{\sigma}\hat{a}^\dagger), \quad (16)$$

where $\delta \equiv \omega_0 - \omega$ is the detuning. Our method applies to both the dispersive and the resonant regime.

Dispersive interaction

We assume first a dispersive interaction, with $|\delta| \gg \Omega_0\sqrt{n}$, i.e., the frequency of the field ω is far detuned from the transition frequency ω_0 of the TLS, and we assume that the atom has three relevant states $|g\rangle$, $|e\rangle$, and $|i\rangle$, so that the field in the high- Q cavity couples dispersively with the states $|g\rangle$ and $|i\rangle$, while transitions involving $|e\rangle$ can be neglected. A similar level scheme was adopted in Ref. [26]. We start with the atom in the state $|g\rangle$ and the field in the cavity in a large-amplitude coherent state $|\alpha\rangle$. Before the atom enters into the high- Q cavity it passes through a low- Q cavity and suffers a resonant $\pi/2$ pulse, so it evolves into $U_{\pi/2}|g\rangle = (|e\rangle + |g\rangle)/\sqrt{2}$. The interaction time between the atom and the field in the high- Q cavity may be adjusted by atomic velocity selection and Stark-shifting the atomic levels, so that the interaction ceases when these levels become highly detuned from the cavity mode [39]. In this way, the interaction time T up to the middle of the cavity is adjusted so that $\Omega_0^2 T/4\delta = \pi$, where $\delta = \omega_{ie} - \omega$ is the detuning between

the frequency of the field in the cavity, ω , and the frequency ω_{ie} of the transition $g \leftrightarrow i$. Therefore, $\hat{U}_{JC}(T)|g, \alpha\rangle = |g, -\alpha\rangle$, while the state $|e, \alpha\rangle$ remains the same. The state of the system right before the application of the perturbation is $|\Psi\rangle = \hat{U}_{JC}(T)\hat{U}_{\pi/2}|g, \alpha\rangle$, and reads

$$|\Psi\rangle = (|e, \alpha\rangle + |g, -\alpha\rangle)/\sqrt{2}. \quad (17)$$

Assume now a displacement perturbation, corresponding to the unitary operation $\hat{U}_s = \hat{D}(\beta)$, with $\beta = i\alpha s/|\alpha|$ and $|\beta| = s \ll 1$, is applied to this state. Displacements of the cavity field can be induced by injecting into the cavity coherent fields, produced for instance by a microwave generator, while in the ion-trap setting they can be generated by forces that displace the equilibrium position of the ion. For detecting a small rotation, we first apply the displacement operator $\hat{D}(\alpha)$, during a time $\Delta t \ll T$, which leads to the state

$$|\Psi\rangle = (|e, 2\alpha\rangle + |g, 0\rangle)/\sqrt{2}. \quad (18)$$

A small rotation $\hat{R}(\theta)$ of the cavity field can be implemented by a percussive dislocation of one of the mirrors of the cavity, thus changing the frequency of the mode by a small amount during a small time interval. Alternatively, one may send through the cavity a fast atom, which interacts dispersively with the field, and follows a trajectory that avoids the interaction with the first atom. In the ion-trap context, the same kind of perturbation can be implemented by slightly changing the frequency of the harmonic trapping potential. Note that for the state in Eq. (17) the overlap function $|\langle\Psi|\hat{D}(\beta)|\Psi\rangle|^2$ is equal to $|\langle\text{cat}_2|\text{cat}_2(s)\rangle|^2$ given by Eq. (12). In an analogous way, for the state in Eq. (18) we have $|\langle\Psi|\hat{R}(\theta)|\Psi\rangle|^2 = |\langle\text{cat}_2|\text{cat}_2(\theta)\rangle|^2$, also given by Eq. (12) with $s = \theta|\alpha|$.

After the perturbation is applied, we undo the total unitary evolution $\hat{U}_{JC}(T)\hat{U}_{\pi/2}$ [or $\hat{D}(\alpha)\hat{U}_{JC}(T)\hat{U}_{\pi/2}$ for a rotation perturbation], by letting the atom interact with the cavity field again for a time T . Since T is half the period of the dispersive JC evolution, when the atom leaves the cavity at time $2T$ the JC dynamics is automatically undone. Up to a global phase, the final state is

$$|\Psi_f\rangle = \frac{1}{2}(1 - e^{i4|\alpha|s})|e, \alpha\rangle + \frac{1}{2}(e^{i4|\alpha|s} + 1)|g, \alpha\rangle. \quad (19)$$

For a small rotation θ , we obtain the same final state with the displacement s replaced by $\theta|\alpha|$.

The probabilities that the atom exits the cavity in the upper and lower states depend on the small parameter s (equivalently $\theta = s/|\alpha|$),

$$P_e = 1 - P_g = [1 - \cos(4|\alpha|s)]/2, \quad (20)$$

thus exhibiting the characteristic oscillation associated with the interference pattern of the Wigner function. A good estimate of the unknown parameter s requires repeating the measurement several times. After R repetitions, the probability that the outcome $|e\rangle$ is obtained r times is given by a binomial distribution. In the large- R limit, it is well approximated by a Gaussian distribution in the variable

$\xi = r/R$, which can be regarded as effectively continuous [41]. In this limit the probability distribution for the estimator $\tilde{s} = \arccos(2r/R - 1)/4|\alpha|$ of the true displacement s is [42]

$$P(\tilde{s}) \approx \frac{1}{\sqrt{2\pi\Delta\tilde{s}^2}} e^{-(\tilde{s}-s)^2/2\Delta\tilde{s}^2}, \quad (21)$$

where the uncertainty of \tilde{s} is $\Delta\tilde{s} = 1/8\sqrt{R\bar{n}}$, reaching the Heisenberg precision for displacement since $R\bar{n}$ is the total number of photons used in the measurement.

Resonant interaction

We discuss now the case of resonant coupling, $\delta = 0$. This case has over the dispersive case the advantage of requiring much shorter transit times. The corresponding experimental setup leads to collapses and revivals of the atomic population [43]. We start with an initial product state of the TLS-oscillator composite system $|e, \alpha\rangle$ in which the field coherent state has a mesoscopic mean number of photons $\bar{n} = |\alpha|^2$. The joint evolution of the atom-field system inside the cavity is given by $\hat{U}_{JC} \equiv \exp(-i\hat{H}'_{AF}t/\hbar)$, and it can be calculated following the approach developed in [44]. Since the field in the cavity is a superposition of different number of photon states, the corresponding Rabi frequencies are spread. Therefore, the atom gets entangled with the field in a quantum superposition of two coherent components that rotate in opposite directions in phase space [45]. We set up the velocity of the atom so that the transit time T up to the middle of the cavity is half the revival time $T_R = 4\pi\sqrt{\bar{n}}/\Omega_0$. This transit time is much shorter than the one for the dispersive case. The evolved state $|\Psi\rangle = \hat{U}_{JC}(T)|e, \alpha\rangle$ turns out to be the product state [44,45],

$$|\Psi\rangle = (e^{-i(\pi/2)\bar{n}}|-\alpha\rangle - e^{i(\pi/2)\bar{n}}|i\alpha\rangle)/\sqrt{2} \otimes |\phi\rangle_A, \quad (22)$$

where $|\phi\rangle_A \equiv (1/\sqrt{2})(e^{-i(\pi/2)}|e\rangle + e^{-i\arg(\alpha)}|g\rangle)$.

A small displacement is then applied to the field. At this point the JC dynamics must be inverted. This can be done by a procedure developed in [46]: one applies a percussive controlled phase kick corresponding to the unitary operation $\hat{U}_{\text{kick}} = \hat{\sigma}_z$ that changes the sign of the relative phase between the atomic levels. This amounts to changing the sign of the interaction Hamiltonian ($\hat{\sigma} \rightarrow -\hat{\sigma}$), so the phase kick mimics the time-reversal operation. This idea was experimentally implemented in cavity QED [47] and can be similarly applied in the context of ion traps. The final state $|\Psi_f\rangle = \hat{U}_{JC}^\dagger(T)\hat{D}(\beta)\hat{U}_{JC}(T)|e, \alpha\rangle$, up to a global phase, is

$$|\Psi_f\rangle = \frac{1}{2}(e^{i4|\alpha|s} + 1)|e, \alpha\rangle + \frac{b}{2}(1 - e^{i4|\alpha|s})|g, \alpha\rangle, \quad (23)$$

where $b \equiv e^{-i\arg(\alpha)}$. For small rotations, one proceeds as in the previous case, first displacing the field state in Eq. (22), then applying the rotation, and subsequently inverting the displacement and the time evolution. With the replacement $s \rightarrow \theta|\alpha|$, one gets the same final state (23). Given this final state, one can easily evaluate the probabilities P_e and P_g that the atom exits the cavity in the upper and lower level, and

conclude that also in the case of resonant Jaynes-Cummings interaction one can measure weak forces at the Heisenberg limit.

From an experimental point of view, the resonant case is more convenient than the dispersive one because the interaction times are much shorter. One should also note that, instead of applying the percussive time-inversion pulse, the same result would be obtained by letting the first atom go away of the cavity, after disentanglement, and then sending a second atom, prepared in the “time-inverted” state, obtained from $|\phi\rangle_A$ by changing the sign of the relative phase between the states $|e\rangle$ and $|g\rangle$. Further shortening of the interaction time can be achieved by letting the atom interact with the field for a time $\Delta t < T_R/2$, so that in the intermediate state the atom is entangled with the two coherent states $|\alpha e^{\pm i\phi/2}\rangle$ ($\phi = \Omega_0 \Delta t / 2\sqrt{\bar{n}}$), and then inverting the dynamics. After an equal amount of time, one gets again a state like the one in Eq. (23), with s replaced by $s \sin(\phi/2)$, which implies reduced sensitivity, but does not change the scaling of the minimum detectable displacements and rotations.

Finally, we discuss the viability of experimental demonstration with cavity QED and ion-trap implementations. For cavity QED, one should have the interaction time $T = 2\pi\sqrt{\bar{n}}/\Omega_0$ much smaller than the decoherence time, given for the low temperatures used in typical experiments by $\tau_{\text{cav}}/\bar{n}$, where τ_{cav} is the damping time of the cavity field (this condition is probably too strict, in view of the fact that the maximum distance in phase space between the two coherent components of the cat state, and therefore the maximum decoherence rate, is achieved only when the atom is in the middle of its trajectory). According to this criterium, one should have therefore $\tau_{\text{cav}} \gg 2\pi(\bar{n})^{3/2}/\Omega_0$. For a typical value $\Omega_0 = 3 \times 10^5 \text{ s}^{-1}$ and $\bar{n} = 20$, one gets that $\tau_{\text{cav}} \gg 1.9 \text{ ms}$. This condition is within reach of present techniques in cavity

QED, where damping times of the order of 15 ms can be achieved [48]. Atomic state detection has also been perfected. Present efficiency is between 80% and 100% [49], which should be sufficient to detect the sub-Planck oscillations.

For ions, detection efficiency is close to 100%, but one still has to consider decoherence effects affecting the vibrational cat state. Considering a typical value $2\pi/\Omega_0 = 140 \mu\text{s}$, one gets $T \approx 0.6 \text{ ms}$ for a vibrational state with $\bar{n} = 20$. Assuming a damping time for the center-of-mass motion of 100–200 ms, which is compatible with present experiments [50], the decoherence time for the vibrational cat state would be between 5 and 10 ms, thus satisfying the requirement that it should be much larger than the interaction time T .

CONCLUSIONS

We have shown that sub-Planck quantum phase-space structures [20] have remarkable implications for quantum parameter estimation, as they are responsible for Heisenberg-limited sensitivity to perturbations. We have proposed a general method to measure perturbations with such high sensitivity, coupling a harmonic oscillator with a two-level system. This method was applied to cavity QED and ion-trap settings, which should be within experimental reach.

ACKNOWLEDGMENTS

We are grateful to R. L. de Matos Filho, J. M. Raimond, and A. Smerzi for fruitful discussions. We acknowledge partial support from NSA. F.T. and L.D. acknowledge the support of the program Millennium Institute for Quantum Information and of the Brazilian agencies FAPERJ and CNPq. F.T. thanks Los Alamos National Laboratory for the hospitality during his stay.

-
- [1] For a recent review, see V. Giovannetti, S. Lloyd, and L. Maccone, *Science* **306**, 1330 (2004).
 - [2] A. Gilchrist, K. Nemoto, W. J. Munro, T. C. Ralph, S. Glancy, S. L. Braunstein, and G. J. Milburn, *J. Opt. B: Quantum Semi-classical Opt.* **6**, S828 (2004).
 - [3] B. Yurke, S. L. McCall, and J. R. Klauder, *Phys. Rev. A* **33**, 4033 (1986).
 - [4] J. J. Bollinger, W. M. Itano, D. J. Wineland, and D. J. Heinzen, *Phys. Rev. A* **54**, R4649 (1996).
 - [5] V. B. Braginsky and F. Ya. Khalili, *Quantum Measurements* (Cambridge University Press, Cambridge, U.K., 1992).
 - [6] C. M. Caves, K. S. Thorne, R. W. P. Drever, V. D. Sandberg, and M. Zimmermann, *Rev. Mod. Phys.* **52**, 341 (1980).
 - [7] M. J. Holland and K. Burnett, *Phys. Rev. Lett.* **71**, 1355 (1993).
 - [8] W. J. Munro, K. Nemoto, G. J. Milburn, and S. L. Braunstein, *Phys. Rev. A* **66**, 023819 (2002).
 - [9] L. Pezzé and A. Smerzi, e-print quant-ph/0508158.
 - [10] M. D’Angelo, M. V. Chekhova, and Y. Shih, *Phys. Rev. Lett.* **87**, 013602 (2001).
 - [11] K. Edamatsu, R. Shimizu, and T. Itoh, *Phys. Rev. Lett.* **89**, 213601 (2002).
 - [12] P. Walther, J. W. Pan, M. Aspelmeyer, R. Ursin, S. Gasparoni, and A. Zeilinger, *Nature (London)* **429**, 158 (2004).
 - [13] M. W. Mitchell, J. S. Lundeen, and A. M. Steinberg, *Nature (London)* **429**, 161 (2004).
 - [14] Z. Zhao, Y.-A. Chen, A.-N. Zhang, T. Yang, H. J. Briegel, and J.-W. Pan, *Nature (London)* **430**, 54 (2004).
 - [15] H. S. Eisenberg, G. Khoury, G. Durkin, C. Simon, and D. Bouwmeester, *Phys. Rev. Lett.* **93**, 193901 (2004).
 - [16] H. S. Eisenberg, J. F. Hodelin, G. Khoury, and D. Bouwmeester, *Phys. Rev. Lett.* **94**, 090502 (2005).
 - [17] S. A. Sackett, D. Kielpinski, B. E. King, C. Langer, V. Mayer, C. J. Myatt, M. Rowe, Q. A. Turchette, W. M. Itano, and D. J. Wineland, *Nature (London)* **404**, 256 (2000).
 - [18] V. Meyer, M. A. Rowe, D. Kielpinski, C. A. Sackett, W. M. Itano, C. Monroe, and D. J. Wineland, *Phys. Rev. Lett.* **86**, 5870 (2001).
 - [19] D. Liebfried, M. D. Barrett, T. Schaetz, J. Britton, J. Chiaverini, W. M. Itano, J. D. Jost, C. Langer, and D. J. Wineland, *Science* **304**, 1476 (2004).
 - [20] W. H. Zurek, *Nature (London)* **412**, 712 (2001).

- [21] C. M. Caves, Phys. Rev. D **23**, 1693 (1981).
- [22] U. M. Titulaer and R. J. Glauber, Phys. Rev. **145**, 1041 (1966).
- [23] Z. Bialynicka-Birula, Phys. Rev. **173**, 1207 (1968).
- [24] A. Miranowicz, R. Tanas, and S. Kielich, Quantum Opt. **2**, 253 (1990).
- [25] K. Tara, G. S. Agarwal, and S. Chaturvedi, Phys. Rev. A **47**, 5024 (1993).
- [26] M. Brune, S. Haroche, J. M. Raimond, L. Davidovich, and N. Zagury, Phys. Rev. A **45**, 5193 (1992).
- [27] S. Schneider, H. M. Wiseman, W. J. Munro, and G. J. Milburn, Fortschr. Phys. **46**, 391 (1998).
- [28] J. Janszky, P. Domokos, and P. Adam, Phys. Rev. A **48**, 2213 (1993).
- [29] P. K. Pathak and G. S. Agarwal, Phys. Rev. A **71**, 043823 (2005).
- [30] M. Hillery, R. F. O'Connell, M. O. Scully, and E. P. Wigner, Phys. Rep. **106**, 121 (1984).
- [31] N. L. Balazs and B. K. Jennings, Phys. Rep. **104**, 347 (1984).
- [32] A. M. Ozorio de Almeida, R. O. Vallejos, and M. Saraceno, J. Phys. A **38**, 1473 (2005).
- [33] R. A. Jalabert and H. M. Pastawski, Phys. Rev. Lett. **86**, 2490 (2001).
- [34] Z. P. Karkuszewski, C. Jarzynski, and W. H. Zurek, Phys. Rev. Lett. **89**, 170405 (2002).
- [35] P. Jacquod, I. Adagideli, and C. W. J. Beenakker, Phys. Rev. Lett. **89**, 154103 (2002).
- [36] F. M. Cucchietti, D. A. R. Dalvit, J. P. Paz, and W. H. Zurek, Phys. Rev. Lett. **91**, 210403 (2003).
- [37] D. A. R. Dalvit *et al.* (unpublished).
- [38] E. T. Jaynes and F. W. Cummings, Proc. IEEE **51**, 89 (1963).
- [39] J. M. Raimond, M. Brune, and S. Haroche, Rev. Mod. Phys. **73**, 565 (2001).
- [40] D. J. Wineland, C. Monroe, W. M. Itano, D. Leibfried, B. E. King, and D. M. Meekhof, J. Res. Natl. Inst. Stand. Technol. **103**, 259 (1998).
- [41] A. Luis, Phys. Rev. A **69**, 044101 (2004).
- [42] The only prior information about the signal is that $0 \leq s \leq \pi/4|\alpha| \ll 1$ for displacements, or equivalently $0 \leq \theta \leq \pi/4|\alpha|^2 \ll 1$ for rotations. This is not a restrictive condition since one can set up the value of $|\alpha|$ in the experiment in order for $\pi/4|\alpha|$ to be an upper bound of the expected displacement (or $\pi/4|\alpha|^2$ an upper bound for expected rotations) to be measured.
- [43] J. H. Eberly, N. B. Narozhny, and J. J. Sanchez-Mondragon, Phys. Rev. Lett. **44**, 1323 (1980); S. J. D. Phoenix and P. L. Knight, Ann. Phys. (N.Y.) **186**, 381 (1988); J. Eiselt and H. Risken, Opt. Commun. **72**, 351 (1989); J. Eiselt and H. Risken, Phys. Rev. A **43**, 346 (1991); B. W. Shore and P. L. Knight, J. Mod. Opt. **40**, 1195 (1993).
- [44] J. Gea-Banacloche, Phys. Rev. A **44**, 5913 (1991).
- [45] A. Auffeves, P. Maioli, T. Meunier, S. Gleyzes, G. Nogues, M. Brune, J. M. Raimond, and S. Haroche, Phys. Rev. Lett. **91**, 230405 (2003).
- [46] G. Morigi, E. Solano, B.-G. Englert, and H. Walther, Phys. Rev. A **65**, 040102(R) (2002).
- [47] T. Meunier, S. Gleyzes, P. Maioli, A. Auffeves, G. Nogues, M. Brune, J. M. Raimond, and S. Haroche, Phys. Rev. Lett. **94**, 010401 (2005).
- [48] S. Haroche (private communication).
- [49] P. Maioli, T. Meunier, S. Gleyzes, A. Auffeves, G. Nogues, M. Brune, J. M. Raimond, and S. Haroche, Phys. Rev. Lett. **94**, 113601 (2005).
- [50] R. Blatt (private communication).